Spectroscopic investigation on the inclusion complex formation between amisulpride and γ-cyclodextrin

Jeetendra Singh Negi*, Shivpal Singh

Department of Pharmaceutical Sciences, S Bhagwan Singh PG Institute of Bio-medical Sciences and Research, Balawala, Dehradun 248161, Uttarakhand, India

ARTICLE INFO

ABSTRACT

The purpose of this research was to investigate inclusion complex formation between poorly soluble drug amisulpride (AMI) and γ-cyclodextrin (γ-CD). The solubility of AMI was enhanced by formation of inclusion complex of AMI with nano-hydrophobic cavity of γ-CD. The stoichiometry of inclusion complex was studied by continuous variation Job's plot method and found 1:1. The binding constant was found 1166.65 M^{-1} by Benesi–Hildebrand plot. The molecular docking of AMI and γ-CD was done to investigate complexation. The inclusion complex formation was further confirmed by ^1H NMR and FT-IR, DSC and XRD analysis. The solubility of AMI was increased 3.74 times after inclusion complex formation with γ-CD.

1. Introduction

Cyclodextrins (CDs) are macrocyclic oligosaccharides composed of repeating α-D-glucopyranoside units (Loftsson & Duchene, 2007). Three distinctive classes of CDs are alpha (α), beta (β) and gamma (γ) cyclodextrins having 6, 7 and 8 glucopyranoside units, respectively. The cyclic orientation of these units gives conical or truncated cone structure with a hydrophobic interior and a hydrophilic exterior (Rowe, Sheskey, Weller, & Quinn, 2009). This structure allows CDs to form host–guest inclusion complexes with different sized guest molecules. The chemical stability of guest molecule increases due to the van der Waals attraction, hydrogen bonding and hydrophobic attractions, etc. Due to its wide applicability, CDs used in different areas, such as the cosmetics, food and agro industries. Inclusion complex of CDs have been used in aqueous solubility enhancement of poorly soluble compounds to increase their bioavailability (Brewster & Loftsson, 2007). Amisulpride (AMI) is an atypical antipsychotic drug; effective for treatment of acute and chronic schizophrenic disorders (British Pharmacopoeia, 2009). Like most of the other newer drugs, AMI is also practically insoluble in water. Due to its poor aqueous solubility it gives poor oral bioavailability also (Rosenzweig et al., 2002). Solubility of several drugs has been successfully improved by formation of inclusion complex with cyclodextrins (Cagno, Stein, Basnet, Brandl, & Brandl, 2011; Chen et al., 2011; Misiuk &

Zalewska, 2011). However, in comparison to other types, gamma cyclodextrin (γ-CD) has been utilized for solubility enhancement by very few researchers (Li, Yan, Jiang, & Chen, 2002; Macedo, Andrade, Conegero, & Barreto, 2012; Marcon et al., 2009; Pedesrson, Bjerregaard, Jacobsen, & Sorenson, 1998; Rajagopalan, Chen, & Chow, 1985; Wintgens & Amiel, 2010; Xu, Wang, & Ding, 2011). Among α, β and γ CDs, γ-CD is having largest cavity diameter (0.95 nm) and highest aqueous solubility (23.2 g/100 mL) (Rowe et al., 2009). This work investigates the inclusion complex formation of AMI with γ-CD in order to improve its solubility profile. Due to the bulky structure of AMI molecule, γ-CD was selected for inclusion complex formation.

2. Materials and methods

2.1. Chemicals

AMI was obtained as gift sample from Alchem Lab. Ltd., Mumbai. γ-CD was obtained as gift sample from Jubilient Life Sciences, Noida. Methanol, ortho-dihydrogen phosphate, hydrochloric acid were purchased from CDH Ltd.

2.2. Preparation of amisulpride-γ CD inclusion complex

AMI and γ-CD complex was prepared in a molar ratio of 1:1 by kneading method (Ali, Al-Marzouqi Solieman, Shehadi, & Adem, 2008). Appropriate quantity of γ-CD was dissolved in water and

---

* Corresponding author. Tel.: +91 9458150910.
E-mail address: rx.jnegi@gmail.com (J.S. Negi).

ethanolic solution of AMI was added to it. This mixture was triturated with pestle for 4 h and then placed in dessicator for 48 h.

2.3. Preparation of physical mixture

A physical mixture of AMI and γ-CD in molar ratio of 1:1 was prepared by mixing with spatula in a mortar to obtain homogenous blend.

2.4. Determination of the complexation stoichiometry

Job's method was employed to the determination of the complexation stoichiometry (Nicolazzi, Abdou, Collomb, Marsura, & Finance, 2001; Panichpakdee & Supaphol, 2011). Total molar concentration of AMI and CD aqueous mixture was kept constant at 1.62×10^{-4} M. Only molar ratio was varied from 0 to 1. Absorbance was recorded at different molar ratios by UV spectrophotometer.

2.5. Determination of the Binding constant

The binding constant of AMI-CD inclusion complex was determined by Benesi–Hildebrand equation (Hendy & Breslin, 2011; Srinivasan, Stalin, & Sivakumar, 2012). The concentration of AMI (8.1×10^{-3} M L^{-3}) was kept constant and CD concentration was varied from 0.4×10^{-3} M L^{-3} to 20×10^{-3} M L^{-3}. Following equations were utilized for 1:1 (Eq. (1)) and 1:2 (Eq. (2)) complexation:

$$\frac{1}{A - A_0} = \frac{1}{A' - A_0} + \frac{1}{K(A' - A_0)[\gamma\text{-CD}]} \tag{1}$$

$$\frac{1}{A - A_0} = \frac{1}{A' - A_0} + \frac{1}{K(A' - A_0)[\gamma\text{-CD}]^2} \tag{2}$$

A_0 is the absorption intensity of AMI in the absence of CD, whereas A is the absorption intensity at different CD concentrations. K is the binding constant and calculated from the slope of Benesi–Hildebrand equation using following equation:

$$K = \frac{1}{slope(A' - A_0)} \tag{3}$$

2.6. Molecular docking study

Most probable structure of AMI: γ-CD inclusion complex was determined by molecular docking using Patchdock server (Srinivasan et al., 2012). The 3-D structure of AMI and γ-CD were determined by translating their SMILES formula using CORINA server. Ligand molecule (AMI) was docked into receptor (γ-CD) using PatchDock server. A geometry-based molecular docking algorithm follows by PatchDock server to find the docking transformations having good molecular shape complementarily.

2.7. FT-IR study

FT-IR spectra were obtained by a Perkin-Elmer Paragon 1000 spectrometer. Samples were pressed into KBr pellets and recorded at frequencies from 4000 to 200 cm^{-1}.

2.8. X-ray diffraction (XRD)

XRD studies were performed using a X-ray diffractometer (X'Pert Powder PANalytical system, Netherlands) with Cu Kα radiation generated at 40 mA, 35 kV. Samples were scanned in the range of 5° (2θ) to 50° (2θ).

2.9. Differential scanning calorimetry (DSC)

DSC was carried out using EXSTAR TG/DTA 6300. A mass of 10 mg samples were accurately weighted, sealed in an aluminum pan with nitrogen environment (Nitrogen (200 mL/min)) and equilibrated at 25 °C, which were subjected to a heating run over the temperature range of 25–350 °C.

2.10. NMR spectra

^{1}H NMR spectra of AMI, γ-CD and AMI-γ-CD inclusion complex were recorded using Bruker 500 MHz spectrometer. Samples were dissolved in D$_2$O and degassed by bubbling N$_2$ directly in the NMR tubes. The chemical shifts were reported as ppm and are referenced to the residual water signal.

2.11. Solubility profile of drug and inclusion complex

An excess of drug/complex was dissolved in 20 mL of distilled water and it was shaken for 12 h followed by centrifugation and then the supernatant liquid was diluted suitably and the absorbance was taken at 221 nm.

3. Results and discussion

The inclusion complex formation of AMI with γ-CD in aqueous solution was characterized by UV Spectroscopy. Two spectral bands were observed for AMI at 221 nm and 276 nm whereas no absorption was observed for pure γ-CD in the range of 200–300 nm (Fig. 1a). As the concentration of γ-CD was increased in AMI aqueous solution, the absorption of AMI was also increased at 221 nm and 276 nm. This γ-CD concentration dependent, hyperchromic shift in spectral bands of AMI to higher intensity was resulted due to host guest interaction between γ-CD and AMI (Fig. 1b). Similar changes were also reported by other authors (Gibaud, Zirar, Mutzenhardt, Fries, & Astier, 2005). After reaching a certain limit (0.002 mol L^{-1}) of γ-CD, further increment in γ-CD was not resulted in absorption enhancement of AMI. The stoichiometry of the complex formation between AMI and γ-CD was determined using continuous variation Job's method. The Job's plot is shown in Fig. 2a, where the $R = [\text{AMI}]/\{[\text{AMI}] + [\gamma\text{-CD}]\}$ was varied from 0.1 to 0.9 and plotted against absorbance difference ($\Delta A \times$ mole fraction). As shown in Job's plot the maximum peak was obtained at $R = 0.5$, which indicates the formation of 1:1 inclusion complex between AMI and γ-CD. Because the change in absorbance with increase in concentration of γ-CD was small, the Benesi–Hildebrand method was employed for determination of association constant (Srinivasan et al., 2012). Good correlation ($r^2 = 0.9813$) was obtained for a 1:1 plot (Fig. 2b) of $1/(A - A_0)$ versus $1/[\gamma\text{-CD}]$ whereas nonlinear curve ($r^2 = 0.9014$) was obtained for 1:2 plot (Fig. 2c) of $1/(A - A_0)$ versus $1/[\gamma\text{-CD}]^2$, which also confirms the formation of inclusion complex with 1:1 stoichiometry. The binding constant value K, of 1166.65 M^{-1} was determined using intercept and slope values of 1:1 plot according to Eq. (3). Solubility of AMI in distilled water was found 290.91 ± 16.89 μg/mL whereas solubility of AMI-γ CD inclusion complex was found 1087.68 ± 28.48 μg/mL. Thus, 3.74 times enhancement in solubility was observed for AMI after inclusion complex formation with γ-CD.

The 3D structure of γ-CD and AMI are shown in Fig. 3. Molecular docking has been proven as good tool for complexation investigation (Seridi & Boufelfel, 2011; Yuan, Jin, & Xu, 2012). In this work, PatchDock server was used to dock ligand on receptor. The best probable structure of inclusion complex was generated on the basis of geometric shape complementary score, approximate interface area size and atomic contact energy of complex. For 1:1
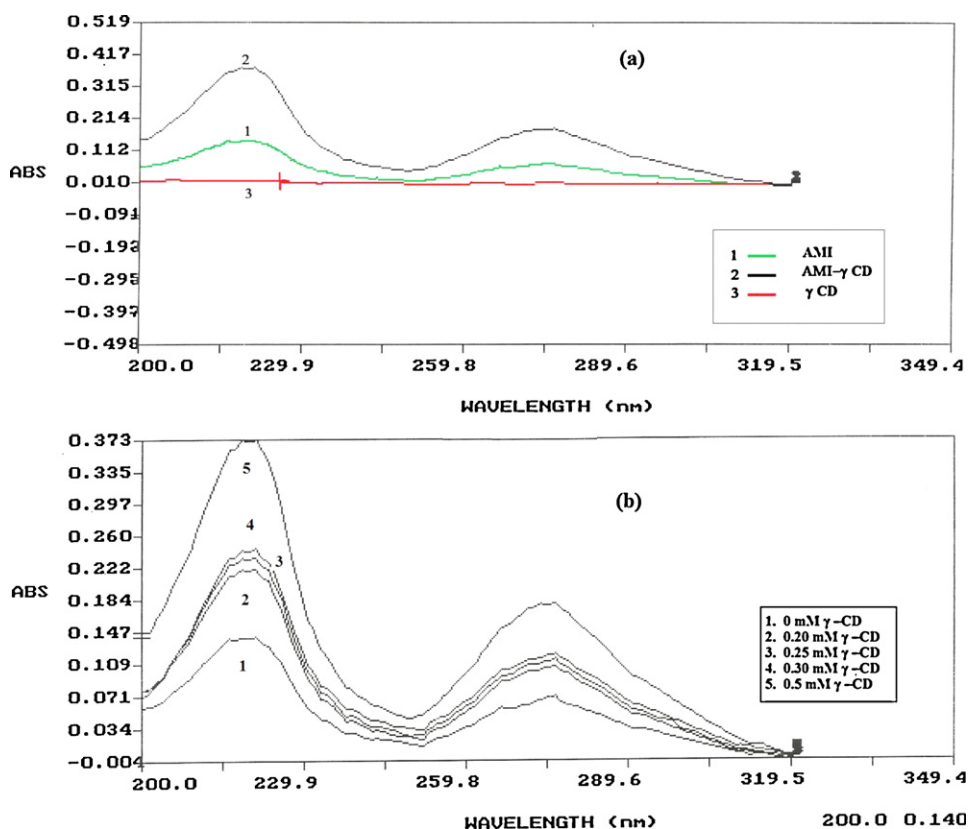
Fig. 1. UV spectra of (a) pure AMI, γ-CD and AMI-γ-CD aqueous solution; (b) AMI and CD solution in increasing CD concentration.

inclusion model the best docked structure of inclusion complex is shown in Fig. 3c. The highest geometric shape complementarity score value, 3976 was obtained for best docked structure. The approximate interface area, 491.50 Å² and atomic contact energy, −360.57 kcal/mol were obtained for highly probable and energetically favorable 1:1 model of inclusion complex. In docked structure only −OCH₃ and −CH₂−CH₃ groups were found outside cavity and other portions were completely occupied inside γ-CD cavity. Sulfone moiety end of AMI was completely dipped inside the γ-CD cavity and pyrrolidine moiety end was entangled with γ-CD chains. In order to confirm complex formation and molecular docking results, AMI-γ CD inclusion complex was evaluated for FTIR, XRD, DSC and NMR studies.

FTIR spectrum of AMI and γ-CD are shown in Fig. 4a and b and Table 1. The FTIR spectrum of AMI was characterized by presence of peaks for amine group, sulfone group, amide group, aromatic

skeleton vibration and methyl group. Broad characteristic OH stretching at 3389.66 cm⁻¹ was present in γ-CD spectrum. Other important peaks of γ-CD were C−O−C stretching, C−C−O stretching, C−H bending and OH bending (Heise, Kuckuk, Bereck, & Riegel, 2010). All the characteristic peaks of AMI and γ-CD were also present in physical mixture of AMI and γ-CD spectrum as shown in Table 1 and Fig. 4c and d. However several AMI peaks were either absent or shifted which suggested change in environment due to inclusion complex formation between AMI and γ-CD. FTIR bands of amine, amide and pyrrole stretching were absent in AMI-γ CD inclusion complex spectrum. The O−H stretching of pure γ-CD shifted to low frequency of 3363.11 cm⁻¹ after inclusion complex formation. This might be due to involvement of γ-CD hydroxyl groups in hydrogen bonding with AMI groups. Aromatic skeleton band was also absent from inclusion complex spectrum which suggests entrapment of aromatic ring inside
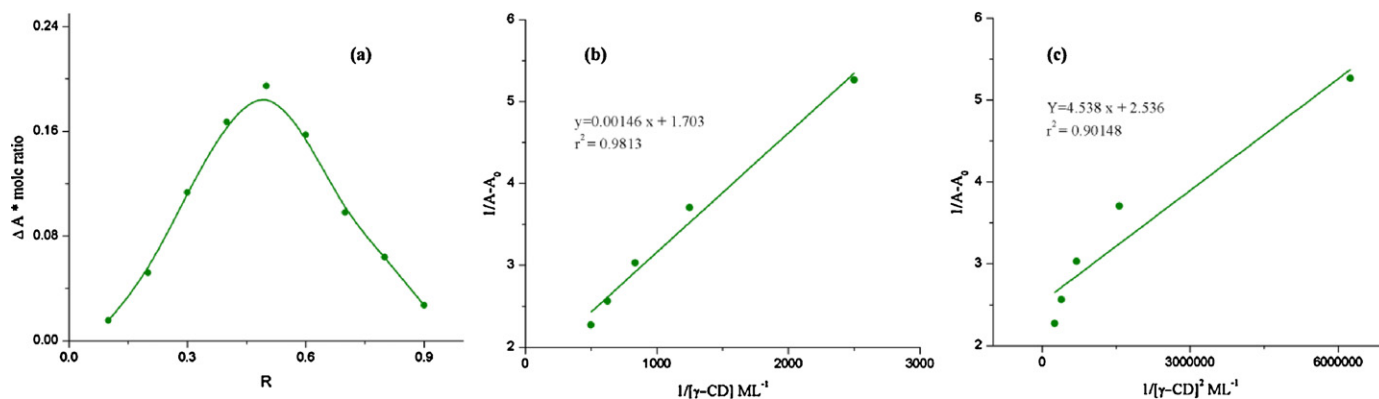

Fig. 2. (a) Job's plot for different molar ratio of AMI and γ-CD, (b) Benesi–Hildebrand plot of $1/(A − A_0)$ versus $1/[γ$-CD] and (c) $1/(A − A_0)$ versus $1/[γ$-CD]².
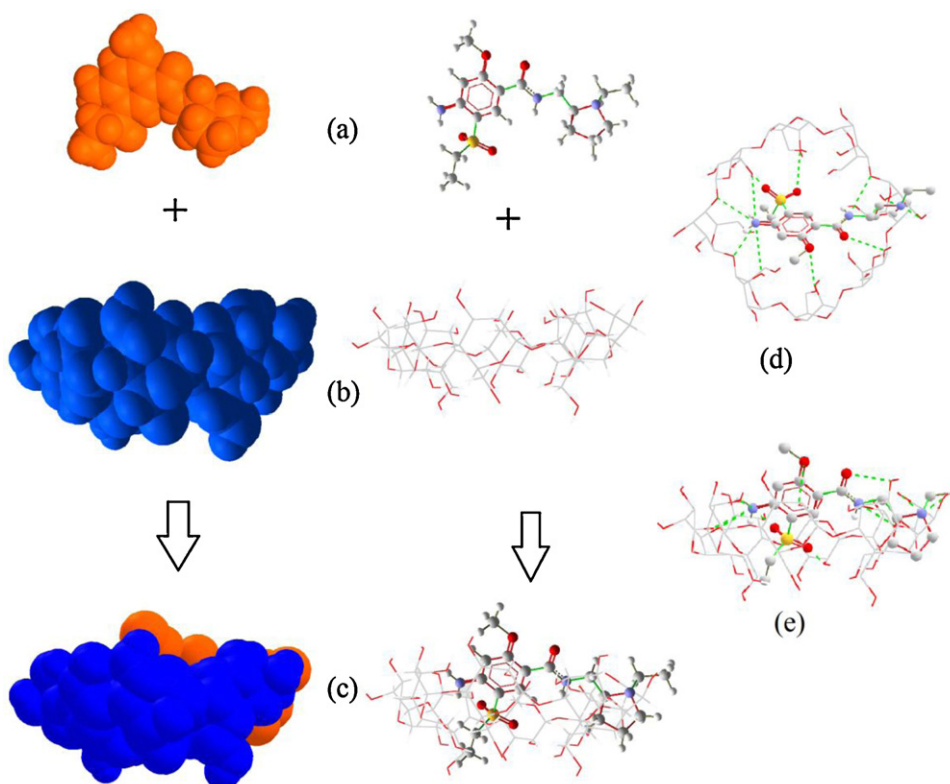
Fig. 3. (a) AMI spacefill and stick-ball structure, (b) γ-CD spacefill and stick-ball structure, (c) best docked structure, (d) Arial view, and (e) interaction possibilities in docked structure.

Table 1
Wavenumbers from FTIR spectra of AMI, γ-CD, physical mixture and AMI-γ-CD inclusion complex.

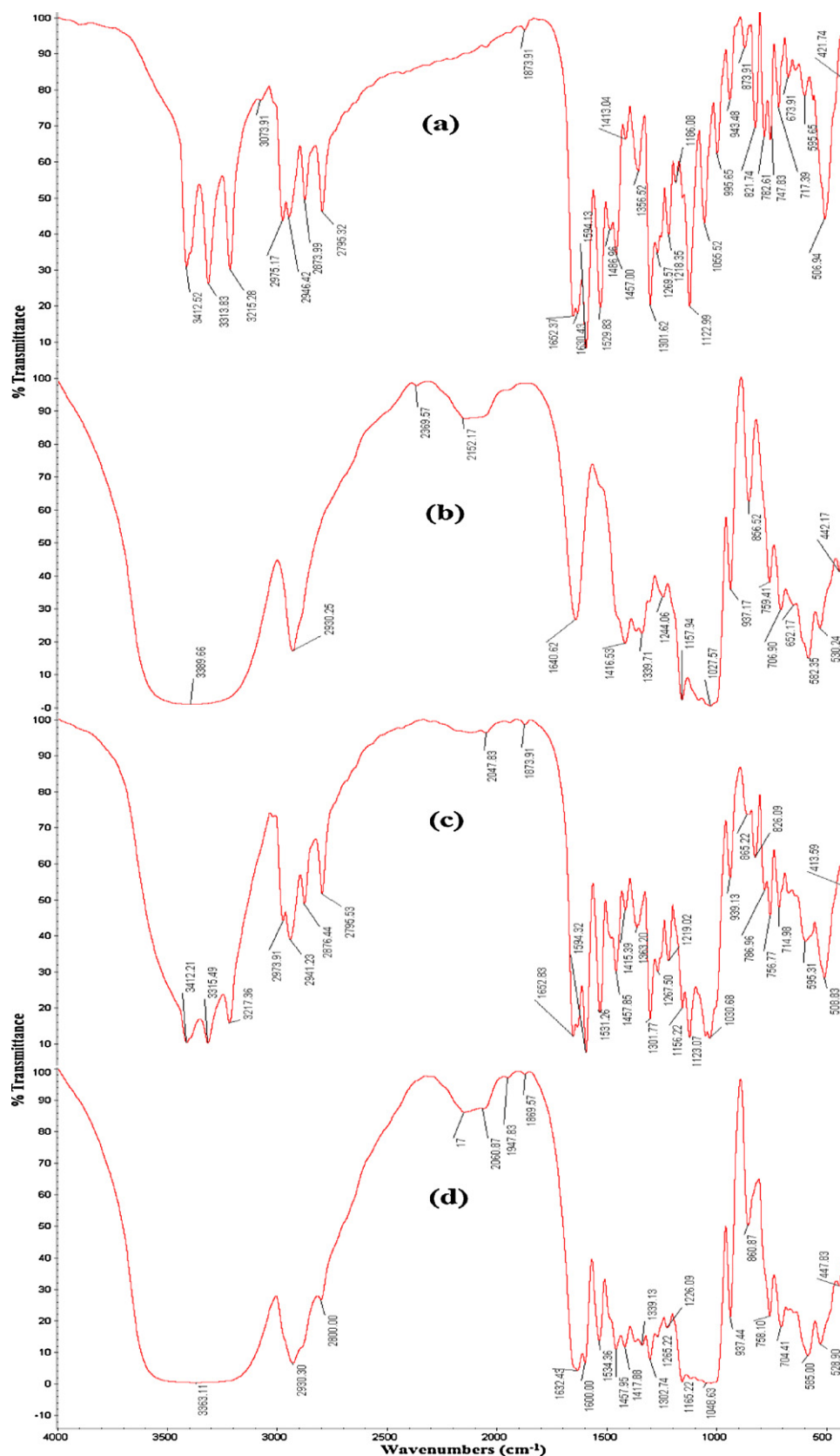| AMI	γ-CD	Physical mixture	AMI-γ-CD inclusion complex
1. 3412.52, 3313.83, 3215.28 cm^{-1}: N—H stretching (v_{as}; v_s) of primary amine, pyrrole and secondary amide 2. 1301.62 cm^{-1}: v(C—N) from aromatic amine 3. 1356.52 cm^{-1}: v_{as} from sulfone group 4. 1122.99 cm^{-1}: v_s from sulfone group 5. 1652.37 cm^{-1}: v(C=O) secondary amide 6. 1529.83 cm^{-1}: δ(N—H) from 2^0 amide 7. 1630.43 cm^{-1}: δ(N—H) from 1^0 amine 8. 1594.13 cm^{-1}: v(C—C) aromatic skeletal vibration 9. 2975.17 and 2873.99 cm^{-1}: v_{as}, v_s (C—H) from CH$_3$ 10. 2946.42 and 2795.32 cm^{-1}: v_{as}, v_s (C—H) from CH$_2$ 11. 1486.96 and 1269.57 cm^{-1}: δ_{as}, τ_s (C—H) of CH$_2$ 12. 1457 and 1413.04 cm^{-1}: δ_{as}, δ_s (C—H) bending from CH$_3$	1. 3389.66 cm^{-1}: v_{as}; v_s of OH 2. 2930.25 cm^{-1}: v_{as} (C—H) from CH$_2$ 3. 1416.53 cm^{-1}: δ_{as} (C—H) from CH$_2$ 4. 1339.71 cm^{-1}: coupled δ_s (C—H) of CH$_2$; δ O—H 5. 1157.94 cm^{-1}: δ_{as} C—O—C 6. 1027.57 cm^{-1}: v(C—C—O) from C—OH 7. 937.17 cm^{-1}: skeletal vibration involving α-1,4linkage 8. 856.52 cm^{-1}: δ (C—C—H), (C—O), (C—C) from anomeric vibration	1. 3412.21, 3315.49, 3217.36 cm^{-1}: N—H stretching (v_{as}; v_s) of primary amine, pyrrole and secondary amide (AMI) with broad band of OH stretch of γ-CD 2. 2973.91 and 2876.44 cm^{-1}: v_{as}, v_s (C—H) from CH$_3$ (AMI) 3. 2941.23 and 2795.53 cm^{-1}: v_{as}, v_s (C—H) from CH$_2$ (AMI) 4. 1652.83 cm^{-1}: v(C=O) secondary amide (AMI) 5. 1630.43 cm^{-1}: δ(N—H) from 1^0 amine (AMI) 6. 1594.32 cm^{-1}: v(C—C) aromatic skeletal vibration (AMI) 7. 1531.26 cm^{-1}: δ(N—H) from 2^0 amide (AMI) 8. 1486.96 and 1267.5 cm^{-1}: δ_{as}, τ_s (C—H) of CH$_2$ (AMI) 9. 1457.85 and 1415.39 cm^{-1}: δ_{as}, τ_s (C—H) of CH$_3$ (AMI) 10. 1301.77 cm^{-1}: v(C—N) from aromatic amine (AMI) 11. 1363.2 and 1123.07 cm^{-1}: v_{as}, v_s from sulfone group (AMI) 12. 1156.22 cm^{-1}: δ_{as} C—O—C (γ-CD) 13. 1030.68 cm^{-1}: v(C—C—O) from C—OH (γ-CD) 14. 939.13 cm^{-1}: skeletal vibration involving α-1,4linkage (γ-CD) 15. 865.22 cm^{-1}: δ(C—C—H), (C—O), (C—C) from anomeric vibration (γ-CD)	1. 3363.11 cm^{-1}: v_{as}; v_s of OH (γ-CD) 2. 2930.30 cm^{-1}: v_{as} (C—H) from CH$_2$ 3. 1632.43 cm^{-1}: v(C=O) secondary amide (AMI) 4. 1600 cm^{-1}: δ(N—H) from 1^0 amine (AMI) 5. 1486.06 and 1265.22 cm^{-1}: δ_{as}, τ_s (C—H) of CH$_2$ (AMI) 6. 1457.95 and 1417.88 cm^{-1}: δ_{as}, τ_s (C—H) of CH$_3$ (AMI) 7. 1339.13 cm^{-1}: v_{as} from sulfone group (AMI) 8. 1302.74 cm^{-1}: v(C—N) from aromatic amine (AMI) 9. 1165.22 cm^{-1}: δ_{as} C—O—C (γ-CD) 10. 1048.83 cm^{-1}: v(C—C—O) from C—OH (γ-CD) 11. 937.44 cm^{-1}: skeletal vibration involving α-1,4linkage (γ-CD) 12. 860.87 cm^{-1}: δ(C—C—H), (C—O), (C—C) from anomeric vibration (γ-CD)

Fig. 4. FTIR spectra of (a) AMI, (b) γ-CD, (c) physical mixture and (d) AMI–γ-CD inclusion complex.

γ-CD cavity. Further sulfone group peaks were also shifted to lower wavenumber which indicates probability of hydrogen bonding with γ-CD. Asymmetric and symmetric stretching of CH$_3$ group of AMI was presented at 1457 and 1413.04 cm^{-1}. These peaks were also presented in inclusion complex spectrum at 1457.85 and 1415.39 cm^{-1}. This indicates CH$_3$ group environment was not changed after inclusion complex formation. These results are in conformity with molecular docking results where AMI
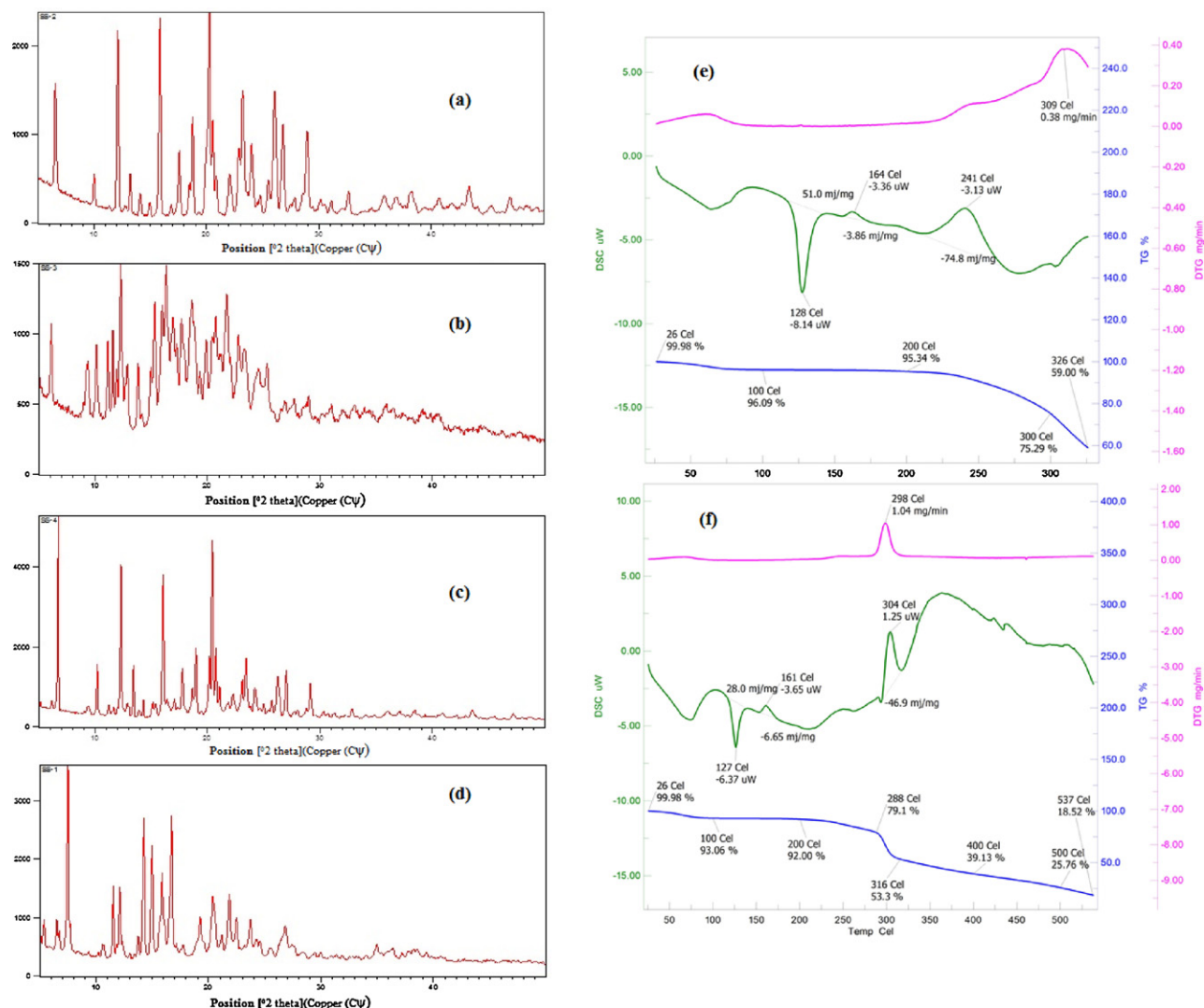
Fig. 5. XRD patterns of (a) AMI, (b) γ-CD, (c) physical mixture, (d) AMI-γ-CD inclusion complex and thermal profile of (e) physical mixture and (f) AMI-γ-CD inclusion complex.

molecule was completely included inside cavity except methyl groups.

XRD patterns of AMI, γ-CD, physical mixture and AMI-γ CD inclusion complex are shown in Fig. 5. Diffraction pattern of bulk AMI was characterized by sharp peaks at 12.13, 15.85, 17.61, 18.77, 20.27, 26.07, 26.83 and 28.97 *2θ*. This pattern suggested highly crystalline nature of AMI. Similarly γ-CD diffraction pattern was characterized by distinctive peaks at 11.6, 13.80, 14.95, 16.34, 19.31, and 21.70 *2θ*. All the individual peaks of AMI and γ-CD were also present in diffraction pattern of physical mixture of AMI and γ-CD contains. The intensity of different peaks was comparatively higher in physical mixture pattern. The intensity of peaks at 12.13, 15.85 and 20.27 *2θ* of AMI were reduced significantly in AMI-γ CD inclusion complex diffraction pattern which suggested reduction in crystallinity of AMI (Fig. 5d) (Hamdi, Abderrahim, & Meganem, 2010). Some low intensity peaks of AMI at 23.23, 23.98 *2θ* were became absent after complexation. This different pattern might be due to inclusion of AMI molecule into cavity of γ-CD. Further, new intense diffraction peaks were also observed at 7.5, 14.24, 16.73, 24 *2θ* for AMI-γ CD inclusion complex which indicates change in AMI and γ-CD environment after inclusion complexation.

In thermo gravimetric analysis (TGA) curve of γ-CD and AMI physical mixture, decomposition of γ-CD was started at 300 °C

whereas in inclusion complex TGA curve, decomposition of γ-CD was started at 288°C (Fig. 5e and f). Remaining weight for physical mixture was 59% at 326 °C and 53% for complex at 316 °C. This change in decomposition behavior suggested change in environment of γ-CD after inclusion complex formation. In differential thermo-gravimetric (DTG) curve, the maximum decomposition rate for physical mixture and complex were obtained at 309 °C and 298 °C, respectively. Similar reduction in maximum decomposition peak was also observed by Macedo et al. after complex formation. Finally, the characteristic melting point of AMI was found at 128 °C in DSC of physical mixture which shifted to lower melting point 127 °C after complex formation (Fig. 5). The intensity of AMI melting endotherm was also reduced with complex formation which suggested reduction in crystallinity of AMI after complex formation. Similar results have been observed by other authors (Kayaci & Uyar, 2012; Roik & Belyakova, 2011).

^{1}H NMR results of pure AMI, γ-CD and AMI-γ CD inclusion complex are shown in Fig. 6. The shift of delta value of γ-CD is given in Table 2 (Ding, He, Huang, & Lu, 2010; Marcon et al., 2009). All the peaks of γ-CD protons were shifted to lower field. This shift might be due to change in environment of γ-CD protons after inclusion complex formation. Shift of delta value of γ-CD toward lower field indicates possibility of both de-shielding effect exerted by
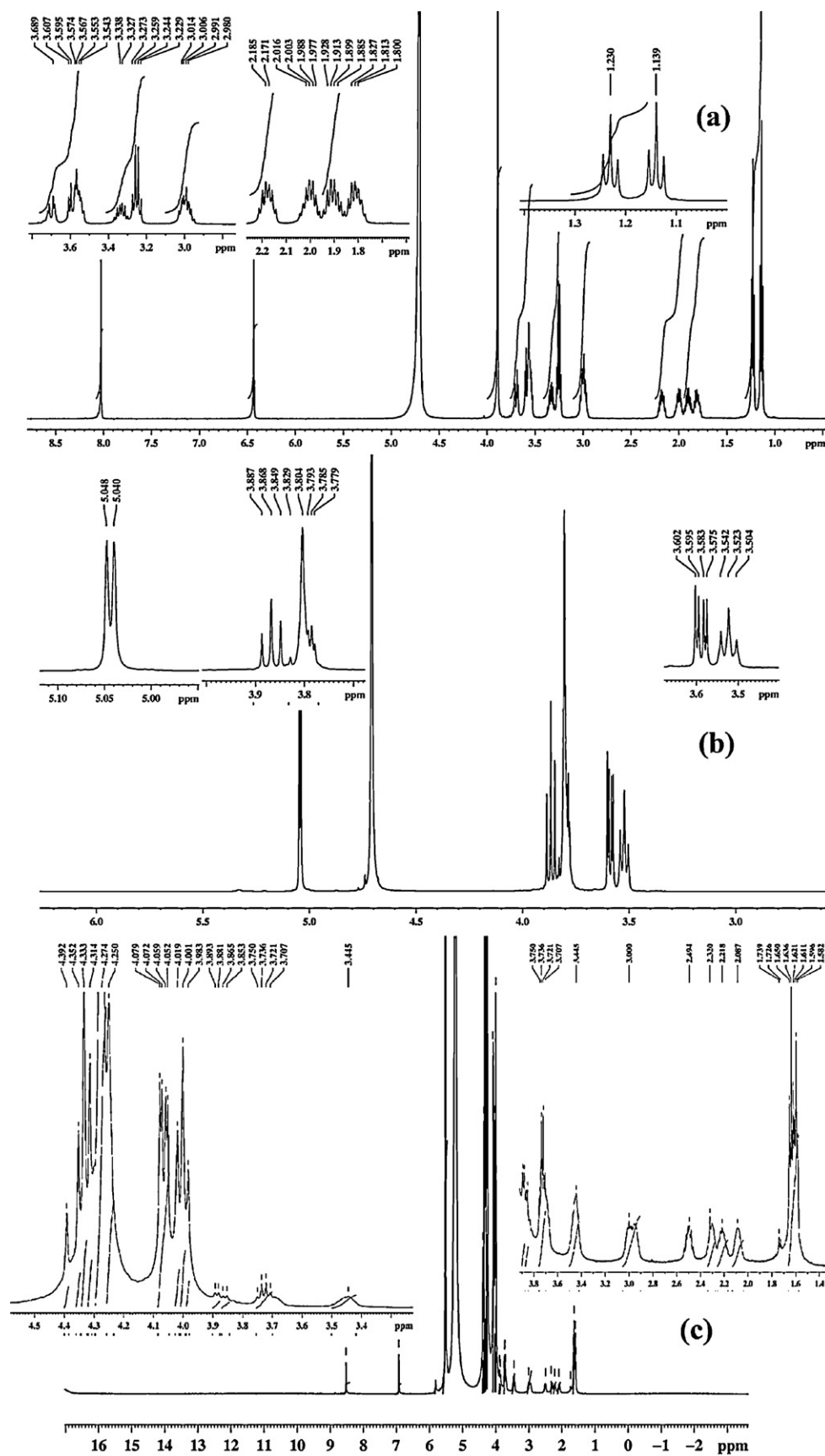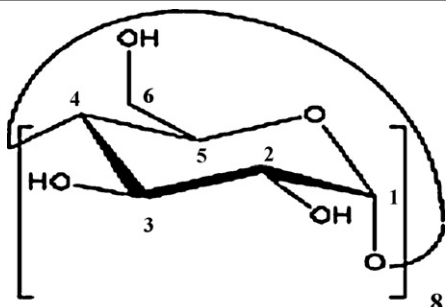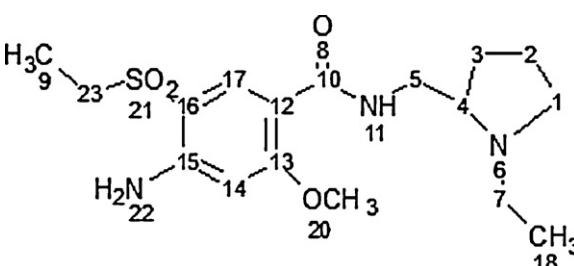
Fig. 6. ^{1}H NMR spectra of (a) AMI, (b) γ-CD and (c) AMI–γ-CD inclusion complex.

Table 2
^{1}H NMR chemical shifts (ppm) for γ-CD, AMI and AMI-γ-CD inclusion complex.

γ-CD

AMI

Proton	γ-CD (δ_0)	AMI-γ-CD inclusion complex (δ)	$\Delta\delta = \delta - \delta_0$	Proton	AMI (δ_0)	AMI-γ-CD inclusion complex (δ)	$\Delta\delta = \delta - \delta_0$
H-4	3.542	4.079	+0.537	18	1.139	1.596	+ 0.457
H-2	3.602	4.072	+0.470	9	1.23	1.636	+ 0.406
H-5	3.779	4.250	+0.471	2	1.928	2.218	+ 0.290
H-6	3.8	4.274	+0.474	3	2.185	2.494	+ 0.309
H-3	3.887	4.392	+0.505	1	3.014	3	-0.014
H-1	5.048	5.515	+0.467	7	3.273	3.445	+0.172
				5	3.574	3.721	+0.147
				11	3.607	3.75	+0.143
				23	3.689	3.865	+0.176
				20	3.89	3.893	+0.003
				22	6.435	6.925	+0.490
				17	8.027	8.525	+0.498

aromatic part (ring current effect) of AMI as well as hydrogen bond formation. In diamagnetic anisotropy, the ring current effect was resulted in shielding of protons below and above aromatic ring and de-shielding of co-planer protons. Several authors reported shielding of H3 and H5 protons of β and HP-β-CD due to ring current effect because of perpendicular positioning of drugs aromatic ring with cyclodextrin molecule cavity (Ding et al., 2010; Yuan et al., 2012). As previously shown in molecular docking results, the aromatic ring of AMI molecule was remained in co-planner position with γ-CD cavity. This co-planner de-shielding by aromatic ring was resulted in shift of γ-CD protons toward lower field. Further delta value shift of AMI also compared and given in Table 2. Delta value of methyl proton attached with sulfone groups was changed significantly. This shift indicates methyl proton was completely occupied inside cavity which means sulfone group was also kept deep inside γ-CD cavity. Similarly delta values for pyrrolidine methylene groups were also changed significantly which suggests interaction of pyrrolidine ring with γ-CD. The delta value of —OCH$_3$ group was not changed even after complex formation, which suggests this part of drug was remained outside the γ-CD cavity. These results were in agreement with molecular docking results where whole AMI molecule was entrapped inside γ-CD cavity, except —OCH$_3$ group.

4. Conclusions

The possibility of the inclusion complex between γ-CD and AMI in aqueous solution was investigated. The effect of γ-CD presence on shift of maximum wavelength was observed by spectroscopic technique. The solubility of poorly soluble drug AMI was enhanced by three-fold after inclusion complex formation. The possibility of 1:1 inclusion complex formation was confirmed by molecular docking using PatchDock server. Further ^{1}H NMR and FTIR analysis confirmed the inclusion complex formation with its structural details. In XRD and DSC analysis, reduction in crystallinity was observed after inclusion complex formation. These results suggested that large cavity of γ-CD can form inclusion complex with bulky molecule like AMI for improvement in its solubility profile.

Appendix A. Supplementary data

Supplementary data associated with this article can be found, in the online version, at http://dx.doi.org/10.1016/j.carbpol.2012.11.082.

References

Ali, H., Al-Marzouqi Solieman, A., Shehadi, I., & Adem, A. (2008). Influence of the preparation method on the physicochemical properties of econazole-β-cyclodextrin complexes. *Journal of Inclusion Phenomena and Macrocyclic Chemistry*, 60, 85–93.

Brewster, M. E., & Loftsson, T. (2007). Cyclodextrin as pharmaceutical solubilizers. *Advanced Drug Delivery Review*, 59, 645–666.

British Pharmacopoeia (2009). London: The Stationary Office (pp. 313–316).

Cagno, M. D., Stein, P. C., Basnet, N. S., Brandl, M., & Brandl, A. B. (2011). Solubilization of ibuprofen with β-cyclodextrin derivatives: Energetic and structural studies. *Journal of Pharmaceutical and Biomedical Analysis*, 55, 446–451.

Chen, W., Yang, L. J., Ma, S. X., Yang, X. D., Fan, B. M., & Lin, J. (2011). Crassicauline A/β-cyclodextrin host–guest system: Preparation, characterization, inclusion mode, solubilization and stability. *Carbohydrate Polymers*, 84, 1321–1328.

Ding, L., He, J., Huang, L., & Lu, R. (2010). Studies on a novel modified β-cyclodextrin inclusion complex. *Journal of Molecular Structure*, 979, 122–127.

Gibaud, S., Zirar, S. B., Mutzenhardt, P., Fries, I., & Astier, A. (2005). Melarsoprol–cyclodextrins inclusion complexes. *International Journal of Pharmaceutics*, 306, 107–121.

Hamdi, H., Abderrahim, R., & Meganem, F. (2010). Spectroscopic studies of inclusion diammonium dipicrate. *Spectrochimica Acta A: Molecular and Biomolecular Spectroscopy*, 75, 32–36.

Heise, H. M., Kuckuk, R., Bereck, A., & Riegel, D. (2010). Infra red spectroscopy and Raman spectroscopy of cyclodextrin derivatives and their ferrocene inclusion complexes. *Vibrational Spectroscopy*, 53, 19–23.

Hendy, G. M., & Breslin, C. B. (2011). A spectrophotometric and NMR study on the formation of an inclusion complex between dopamine and a sulfonated cyclodextrin host. *Journal of Electroanalytical chemistry*, 661, 179–185.

Kayaci, F., & Uyar, T. (2012). Encapsulation of vanillin/cyclodextrin inclusion complex in electrospun polyvinyl alcohol (PVA) nanowebs: Prolonged shelf life and high temperature stability of vanillin. *Food Chemistry*, 133, 641–649.

Li, J., Yan, D., Jiang, X., & Chen, Q. (2002). Formation of the crystalline inclusion complex between γ-CD and poly(N-acetylethylenimine). *Polymer Journal*, *43*(9), 2625–2629.

Loftsson, T., & Duchene, D. (2007). Cyclodextrins and their pharmaceutical applications. *International Journal of Pharmaceutics*, *329*(1), 1–11.

Macedo, O. F. L., Andrade, G. R. S., Conegero, L. S., & Barreto, L. S. (2012). Physicochemical study and characterization of the trimethoprim/2-hydroxypropyl-γ-cyclodextrin inclusion complex. *Spectrochimica Acta A: Molecular and Biomolecular Spectroscopy*, *86*, 101–106.

Marcon, F., Mathiron, D., Pilard, S., Hurtel, A. S. L., Dubaele, J. M., & Pilard, F. D. (2009). Development and formulation of a 0.2% oral solution of midazolam containing γ-cyclodextrin. *International Journal of Pharmaceutics*, *379*, 244–250.

Misiuk, W., & Zalewska, M. (2011). Spectroscopic investigation on the inclusion interaction between hydroxypropyl-β-cyclodextrin and bupropion. *Journal of Molecular Liquids*, *159*(3), 220–225.

Nicolazzi, C., Abdou, S., Collomb, J., Marsura, A., & Finance, C. (2001). Effect of Complexation with cyclodextrins on the in vitro antiviral activity of Ganciclovir against human cytomegalovirus. *Bioorganic and Medicinal Chemistry*, *9*, 275–282.

Panichpakdee, J., & Supaphol, P. (2011). Use of 2-hydroxypropyl-β-cyclodextrin as adjuvant for enhancing encapsulation and release characteristics of asiaticoside within and from cellulose acetate films. *Carbohydrate Polymers*, *85*, 251–260.

Pedesrson, M., Bjerregaard, S., Jacobsen, J., & Sorenson, A. M. (1998). A genuine clotrimazole γ-cyclodextrin inclusion complex-isolation, antimycotic activity, toxicity and an unusual dissolution rate. *International Journal of Pharmaceutics*, *176*(1), 121–131.

Rajagopalan, N., Chen, S. C., & Chow, W. S. (1985). A study of the inclusion complex of amphotericin-B with γ-CD. *International Journal of Pharmaceutics*, *29*(2), 161–168.

Roik, N. V., & Belyakova, L. A. (2011). Cyclodextrin-based drug stabilizing system. *Journal of Molecular Structure*, *987*, 225–231.

Rosenzweig, P., Canal, M., Patat, A., Bergougnan, L., Zieleniuk, I., & Bianchetti, G. A. (2002). Review of the pharmacokinetics, tolerability and pharmacodynamics of amisulpride in healthy volunteers. *Human Psychopharmacology: Clinical and Experimental*, *17*(1), 1–13.

Rowe, R. C., Sheskey, P. J., Weller, P. J., & Quinn, M. E. (2009). *Handbook of pharmaceutical excipients* (6th ed.). London: The Pharmaceutical Press. (pp. 208–210)

Seridi, L., & Boufelfel, A. (2011). Molecular modeling study of Lamotrigine/β-cyclodextrin inclusion complex. *Journal of Molecular Liquids*, *158*, 151–158.

Srinivasan, K., Stalin, T., & Sivakumar, K. (2012). Spectral and electrochemical study of host–guest inclusion complex between 2,4-dinitrophenol and β-cyclodextrin. *Spectrochimica Acta A: Molecular and Biomolecular Spectroscopy*, *94*, 89–100.

Wintgens, V., & Amiel, C. (2010). Water soluble γ-cyclodextrin polymers with high molecular weight and their complex forming properties. *European Polymer Journal*, *46*(9), 1915–1922.

Xu, D., Wang, X., & Ding, L. (2011). Spectroscopic studies on the interaction of γ-cyclodextrin daunorubicin inclusion complex with herring sperm DNA. *Carbohydrate Polymers*, *83*, 1257–1262.

Yuan, C., Jin, Z., & Xu, X. (2012). Inclusion complex of astaxanthin with hydroxypropyl-β-cyclodextrin: UV, FTIR, ^{1}H NMR and molecular modeling studies. *Carbohydrate Polymers*, *89*, 492–496.